

QUASICRYSTALLINE AND CRYSTALLINE PHASES IN RAPIDLY SOLIDIFIED $\text{Al}_{33}\text{Cu}_{10}\text{Fe}_{24}\text{Ti}_{33}$ ALLOY POWDERS^①

Wu Lijun^{1,2}, Chen Zhenhua³, Hu Wangyu¹, Huang Qizhong³, Zhao Lihua¹

¹ Material Research and Test Center, Hunan University, Changsha 410082

² Laboratory of Atomic Imaging of Solids, Institute of Metal Research,
Chinese Academy of Sciences, Shenyang 110015

³ Research Institute of Non-Equilibrium Materials Science and Engineering,
Center South University of Technology, Changsha 410083

ABSTRACT The structure of $\text{Al}_{33}\text{Cu}_{10}\text{Fe}_{24}\text{Ti}_{33}$ alloy powders has been studied by transmission electron microscope (TEM). In the specimens heated at 800 °C, decagonal quasicrystalline phase (*T* phase) and Al solid solution polycrystals have been found. Moreover, two cubic phases and one hexagonal phase have also been found and determined. One cubic phase (*F*) belongs to FCC lattice with $a = 1.15 \text{ nm}$, the other cubic phase (*B*) belongs to BCC lattice with $a = 0.86 \text{ nm}$. The hexagonal phase (*H*) belongs to hexagonal lattice with $a = 0.74 \text{ nm}$ and $c = 0.48 \text{ nm}$.

Key words quasicrystal crystalline phases $\text{Al}_{33}\text{Cu}_{10}\text{Fe}_{24}\text{Ti}_{33}$ alloy rapidly solidified powders

1 INTRODUCTION

Since the historical discovery of the icosahedral quasicrystalline phase in the rapidly solidified Al-Mn alloy by Shechtman *et al*^[1, 2], many quasicrystalline alloy systems have been found. For example, Ti-Ni-V, Pd-U-Si, Al-Mn-Si, Al-Li-Cu, Ga-Mg-Zn, Fe-Ti, Ni-Ti, Al-Cu-Fe and Al-Cu-Co quasicrystalline alloy systems have been exploited^[3-14]. In order to further expand quasicrystalline alloy system, Chen *et al*^[15] proposed a method to prepare multicomponent quasicrystalline alloys according to the composition additive principle and prepared Al-Cu-Fe-Cr, Al-Cu-Fe-Mn and Al-Cu-Fe-Cr-Mn quasicrystalline alloy powders. Xiao *et al*^[16] found that the rapidly solidified AlCuFeTi, AlMnNiTi, AlMnMgZn, AlCuFeMg and AlCuFeMgZn alloy powders can turn to quasicrystals after heat treatment. The purpose of this paper is to study the structure of $\text{Al}_{33}\text{Cu}_{10}\text{Fe}_{24}\text{Ti}_{33}$ alloy powders by

TEM and to present some new results.

2 EXPERIMENTAL

An $\text{Al}_{33}\text{Cu}_{10}\text{Fe}_{24}\text{Ti}_{33}$ (alloy mole fraction) was prepared from 99% pure starting materials. Rapidly solidified alloy powders were then produced with a RS device developed by Chen *et al*^[15]. The powders obtained have an average particle size of about 15 μm and their cooling rates are estimated to be $10^5 \sim 10^7 \text{ K/s}$. In order to get quasicrystals, some powders were heat-treated isothermally for 1 h at 800 °C. The powders were uniformly dispersed on the copper grids covered by holey carbon films for TEM (H-800) observation.

3 RESULTS AND DISCUSSION

In the specimens heated at 800 °C, a kind of powder in which there are little granules is observed. Figs. 1 a, b show the bright field

① Received Apr. 10, 1995; accepted Jun. 21, 1995

image and the electron diffraction pattern of the powder. It is obvious that the electron diffraction pattern is composed of polycrystalline rings and diffraction spots. The d values corresponding to the polycrystalline rings are 0.24, 0.20 and 0.14 nm respectively, which are equal to the spacings of the $\{111\}$, $\{200\}$ and $\{220\}$ planes of Al solid solution (FCC lattice, $a = 0.4099$ nm), respectively. Therefore, the polycrystalline rings are caused by Al solid solution polycrystals. The

diffraction spots in Fig. 1b are the pseudo-five-fold electron diffraction pattern of the decagonal quasicrystalline phase (T phase), which indicates that the diffraction spots are caused by the T phase. Fig. 2 is the dark field image formed with the $\{200\}$ ring of the polycrystals. It shows that the little granules in the powder correspond to the polycrystalline rings. That is to say, the little granules in the powder are Al solid solution polycrystals. Therefore, the powder in Fig. 1a

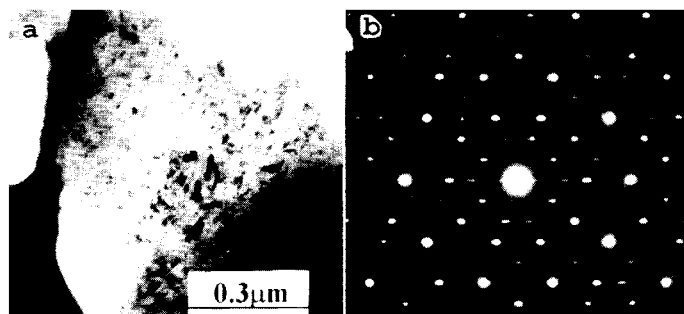


Fig. 1 Bright field image(a) and electron diffraction pattern (b) of the powder with the T phase and the Al solid solution for the specimen heated at 800 °C

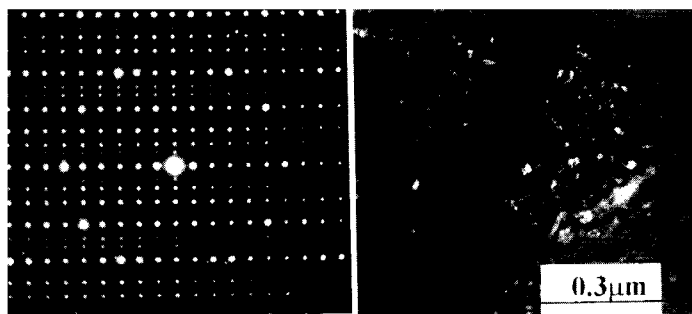


Fig. 2 Dark field image formed with the $\{200\}$ ring of the Al solid solution polycrystals

Fig. 3 Electron diffraction pattern of the T phase taken along two-fold direction

consists of Al solid solution and *T* phase. Fig. 3 is the two-fold electron diffraction pattern of *T* phase taken from the powder without Al solid solution polycrystals, which further verifies the existence of the *T* phase. In addition to the Al solid solution and the *T* phase, another kind of powder is observed. Figs. 4a, b show the bright field image and the dark field image of the powder, respectively. By tilting the powder, many electron diffraction patterns can be obtained. Fig. 5 shows four pieces of electron diffraction patterns, in which, *a*, *b*, *c* and *d* contain the same row of diffraction spots and are indexed along the $[\bar{1}10]^*$ direction. The rotated angles from *a* to *b*, *c*, and *d* are 25.2° , 54.7° and 90° , respectively. From these electron diffraction patterns, the reciprocal space can be constructed as shown in Fig. 6. It is obvious that there are two reciprocal unit cells. One reciprocal unit cell is the BCC reciprocal unit cell. The real unit cell corresponding to this reciprocal unit cell is FCC unit cell with $a = 1.15 \text{ nm}$. We name it the *F* phase. The other reciprocal unit cell is the FCC reciprocal unit cell. The real unit cell corresponding to this reciprocal unit cell is BCC unit cell with $a = 0.86 \text{ nm}$. We name it the *B* phase. The electron diffraction patterns in Fig. 5 can be therefore indexed as the $[001]$, $[\bar{1}13]$, $[\bar{1}11]$ and $[\bar{1}10]$ electron diffraction patterns of the *F* phase and the *B* phase, respectively. The dark field image in Fig. 4b is obtained with the $4\bar{2}2_F$ diffraction spot, which confirms that the powder is composed of the *F* phase and the *B* phase. In fact, the *F* phase and the *B* phase often exist together and the same electron diffraction patterns with those of Fig. 5 can be obtained by tilting the specimens. This indicates that there is steady orientation relationship between the *F* phase and the *B* phase. From Fig. 5 and Fig. 6, the orientation relationship between the *F* phase and the *B* phase can be determined as:

$$\begin{aligned} [100]_F &\parallel [100]_B \\ [010]_F &\parallel [010]_B \\ [001]_F &\parallel [001]_B \end{aligned}$$

In the specimens heated at 800°C , we

still observe a kind of powder as shown in Fig. 7. By tilting the specimen, a number of electron diffraction patterns can be obtained. Fig. 8a~c are three pieces of electron diffraction patterns containing the same dense row of diffraction spots (indexed as the $[\bar{1}10]^*$ direction). The rotated angles from *a* to *b* and *c* are 26.9° and 36.9° respectively. From these data, a hexagonal reciprocal unit cell can be constructed as shown in Fig. 8d. The real unit cell corresponding to this reciprocal unit cell is a hexagonal unit cell with $a = 0.74 \text{ nm}$ and $c = 0.48 \text{ nm}$. We name this phase the *H* phase. According to the lattice data of the *H* phase, the electron diffraction patterns in Fig. 8 can be indexed as the $[001]$, $[113]$ and $[112]$ electron diffraction patterns of the *H* phase, respectively. In fact, in the rapidly solidified $\text{Al}_{33}\text{Cu}_{10}\text{Fe}_{24}\text{Ti}_{33}$ alloy powders, the Al solid solution, the *F* phase, the *B* phase and the *H* phase are all observed. In addition, the amorphous powders are observed. Figs. 9 a, b are the bright field image and the electron diffraction pattern of the amorphous powder in the rapidly solidified specimens. Because the amorphous vanishes when the specimens are heated to 800°C and the morphology of the amorphous is similar to that of the *T* phase except little granules of the Al solid solution, we therefore think that the amorphous may transform into the *T* phase and the Al solid solution when the specimens are heated to 800°C . Further studies on the composition of the *T* phase, the Al solid solution, the *F* phase, the *B* phase and the *H* phase and the relationship between these phases will be done afterwards.

4 CONCLUSIONS

(1) In the specimens heated at 800°C , the *T* phase and the Al solid solution are observed and they may be transformed from the amorphous in the rapidly solidified specimens.

(2) Two cubic phases are found and determined. Cubic phase *F* belongs to FCC lattice with $a = 1.15 \text{ nm}$, cubic phase *B* belongs to BCC lattice with $a = 0.86 \text{ nm}$.

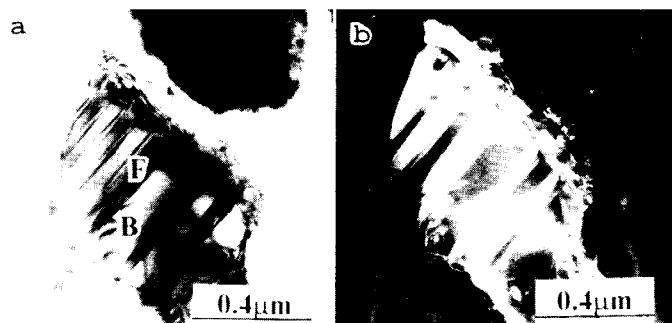


Fig. 4 Morphology of the *F* phase and the *B* phase

(a)—Bright field image; (b)—Dark field image formed with the 422_F diffraction spot

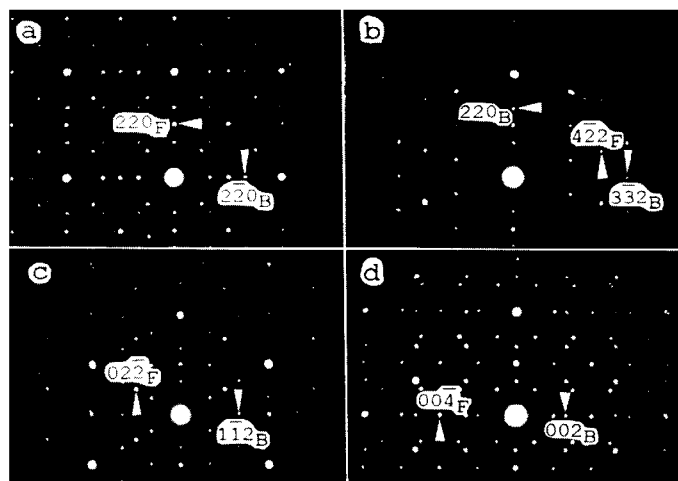


Fig. 5 Electron diffraction patterns of the *F* phase and the *B* phase

(a)— $[001]$; (b)— $[113]$; (c)— $[111]$; (d)— $[110]$

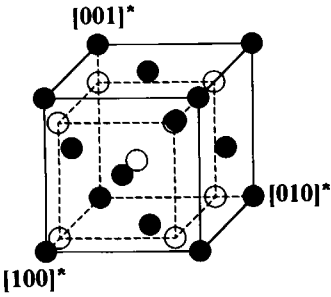


Fig. 6 Reciprocal space of the *F* phase and the *B* phase
○ the *F* phase, ● the *B* phase

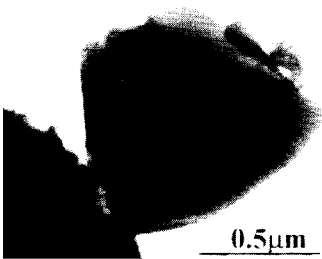


Fig. 7 Bright field image of the *H* phase

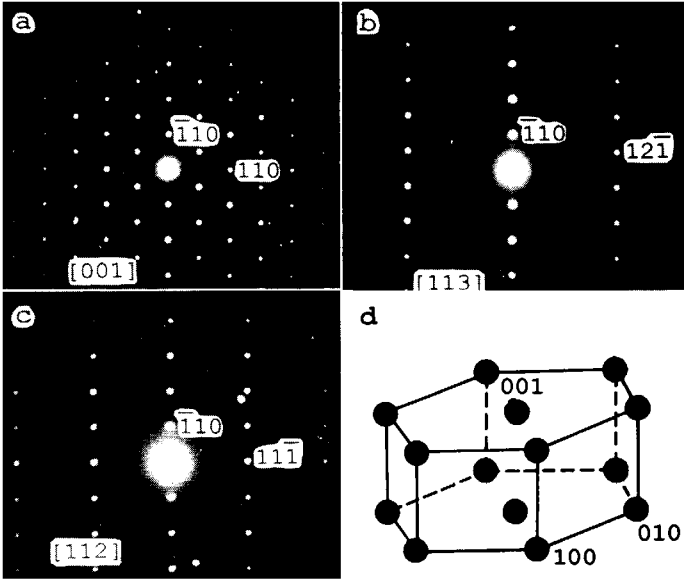


Fig. 8 Electron diffraction patterns and reciprocal unit cell of the *H* phase
(a) $[001]$; (b) $[\bar{1}13]$; (c) $[\bar{1}12]$; (d) —reciprocal unit cell

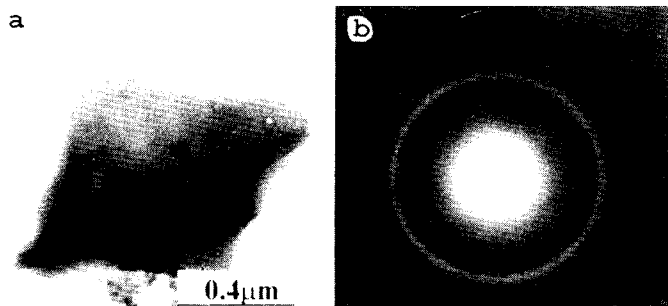


Fig. 9 Bright field image (a) and electron diffraction pattern (b) of the amorphous in the rapidly solidified specimen

(3) A hexagonal phase is found and determined. It belongs to hexagonal lattice with $a = 0.74 \text{ nm}$ and $c = 0.48 \text{ nm}$.

REFERENCES

- 1 Shechtman D, Blech I A, Gratias D, Chan J W. Phys Rev Lett, 1984, 53: 1951.
- 2 Shechtman D, Blech I A. Met Trans, 1985, 16: 1005.
- 3 Zhang Z, Ye H Q, Kuo K H. Phil Mag, 1985, A52: 249.
- 4 Poon S J, Drehman A J, Lawless K R. Phys Rev Lett, 1985, 55: 21.
- 5 Elser V, Henley C L. Phys Rev Lett, 1985, 55: 2883.
- 6 Sainfort P, Bubost B. J Phys Paris, 1986, 47: C3-321.
- 7 Ohashi W, Spaepen F. Nature, 1987, 330: 555.
- 8 Dong C, Hei Z K, Wang L B, Song Q H, Wu Y K, Kuo K H. Scripta Metall, 1986, 20: 1155.
- 9 Shen Y, Dmowski W, Egami T, Poon S J, Shiflet G J. Phys Rev B, 1988, 37: 1146.
- 10 Beeli C, Nissen H V, Robadey J. Phil Mag Lett, 1991, 63: 87.
- 11 Tsai A P, Inoue A, Masumoto T. Jpn J appl Phys, 1987, 26: L1505.
- 12 Tsai A P, Inoue A, Masamoto T. J Mater Sci Lett, 1988, 7: 322.
- 13 He L X, Wu Y K, Kuo K H. J Mater Sci Lett, 1988, 7: 1284.
- 14 Tsai A P, Inoue A, Masumoto T. Mater Trans JIM, 1989, 30: 463.
- 15 Chen Zhenghua, Jiang Xiangyang, Wang Yun, Zhou Duosan, Qian Chongliang, Huang Peiyun, Xiao Jueming, Wu Lijun. Scripta Metall, 1992, 26: 291.
- 16 Xiao Jueming, Wu Lijun, Li ChuangPin, Yang Qiaoqin, Chen Zhenhua, Jiang Xiangyang, Wang Yun. J Mat Sci Lett, 1994, 13: 25.

(Edited by Peng Chaoqun)